Hybrid Physics-based and Data-driven Model Predictive Control for Multi-Zone Building's Thermal Comfort Under Disjunctive Uncertainty

Guoqing Hu*, Fengqi You*

**Cornell University, Ithaca, NY, 14850*
USA (e-mail: Fengqi.you@cornell.edu).

Abstract: This paper develops a hybrid approach that utilizes the distributional information of the disjunctive uncertainty sets and incorporates them into the model predictive control (MPC). This approach aims at the multi-zone building control to the thermal comfort, and it's robust to the uncertain weather forecast errors. The control objective is to maintain each zone's temperature and relative humidity within the specified ranges using the minimum cost of energy of the underlying heating system. The hybrid model is constructed using a physics-based and regression method for the temperature and relative humidity of each zone in the building. The uncertainty space is based on historical weather forecast error data, which are captured by a group of disjunctive uncertainty sets using k-means clustering algorithm. Machine learning approaches based on principal component analysis and kernel density estimation are used to construct each basic uncertainty set and reduce the conservatism of resulting robust control action under disturbances. A robust MPC framework is developed based on the proposed hybrid model and data-driven disjunctive uncertainty set. An affine disturbance feedback rule is employed to obtain a tractable approximation of the robust MPC problem. A case study of controlling temperature and relative humidity of a multi-zone building in Ithaca, New York, USA, is presented. The results demonstrate that the proposed hybrid approach can reduce 9.8% to 17.9% of total energy consumption compared to conventional robust MPC approaches. Moreover, the proposed hybrid approach can essentially satisfy the thermal constraints that certainty equivalent MPC and robust MPC largely violate.

Keywords: model predictive control, machine learning, multi-zone building control, hybrid model, uncertainty

NOMENCLATURE

A	System matrix of system states in a compact form
B_u	System matrix of control inputs in a compact form
B_v	System matrix of deterministic disturbances in a compact form
B_w	System matrix of uncertain disturbances in a compact form
c_p	Specific heat of air
F_u	Coefficient matrix for control input constraints in a compact form
F_x	Coefficient matrix for state variable constraints in a compact form
f_u	Coefficient vector for control input constraints in a compact form
f_x	Coefficient vector for state variable constraints in a compact form
$m_{air,t}$	Mass of supply air during the period from time t to time $t + 1$
$m_{dehum,t}$	Mass of water vapor taken by dehumidifier during the period from time t to time $t + 1$
$m_{hum,t}$	Mass of water vapor provided by humidifier during the period from time t to time $t + 1$
$m_{heat,in,t}$	Mass of airflow provided by air circulation during the period from time t to time $t + 1$
$m_{heat,out,t}$	Mass of airflow taken by air circulation during the period from time t to time $t + 1$
Q	Heat energy
RH_t	Relative humidity in the zone at time t
$RH_{out,t}$	Ambient relative humidity at time t
$T_{air,t}$	Ambient temperature at time t
$T_{zone,t}$	Zone temperature at time t
$T_{heat,t}$	Heated air temperature at time t
V_{zone}	Zone volume
ΔT	Temperature difference between heated supply air and ambient
δT	Temperature difference between heated supply air and zone
$\rho_{heat,sat,t}$	Saturated water vapor density at ambient temperature at time t
$\rho_{abs,t}$	Absolute water vapor density at time t
ρ_{air}	Air density
$\rho_{water,sat,t}$	Saturated water vapor density at zone temperature at time t
$\rho_{sat,t}$	Saturated water vapor density at time t

1. INTRODUCTION

The energy demand is ascending along with the growing population in recent years (Shi et al., 2016). Especially 40 % of the total energy production is used for building (Shaikh et al., 2014). According to the EIA report in 2019, heating and humidity control contribute to 30 % of total power consumption, which dominates the needs of typical households. Those data indicate the significant importance of the control of both temperature and humidity.

Many studies on the control of a building's temperature have already been conducted to efficiently use the energy while meeting thermal comfort constraints. In work by Marszal et al. (2011), the zero-energy building was proposed and performed remarkably in the test; however, such a strategy can only be selectively applied to a limited area (D'agostino et al., 2017). PID is also used in controlling the building (Johnson and Moradi, 2005). In contrast, traditional PID tends to demonstrate instabilities and frequent overshoot thermostats in the simulation, resulting in excessive power usage (Kiam Heong et al., 2005; Yun et al., 2006). Model predictive control (MPC), on the other hand, is a powerful approach to controlling the building temperature and has been reported to save a tremendous amount of energy usage compared to the rule-based control strategies (Prívara et al., 2011; Oldewurtel et al., 2012; Ma et al., 2012; Široký et al., 2011; Shang and You, 2019). Nevertheless, much of the research still focuses on single-zone control, which has limited application in real life. Therefore, multi-zone thermal building models are needed to better capture and represent the thermal dynamics within the house and develop effective control methods. Some papers proposed control strategies for the multi-zone building model (Morosan et al., 2011; Yang and Wang, 2013); however, controlling the temperature alone cannot ensure thermal comfort, which is not exclusively contributed by temperature; Relative humidity values should also be highlighted. In work by Zingano (2001), they have highlighted that relative humidity is tightly related to thermal comfort. Humidity is also important for some specialized buildings like greenhouses (Chen and You, 2021, 2022). Besides, the health condition of occupants can no longer be ensured if the improper relative humidity is adjusted (Baughman and Arens, 1996).

In this study, we develop a hybrid approach to multi-zone building's room temperature and relative humidity control under realistic conditions, which is k-mean clustered, principal component analysis (PCA), and kernel density estimation (KDE) based data-driven RMPC (KM-PKDDRMPC). We apply this model to the multi-zone building's hybrid model, which is constructed from the physics-based model, which includes both room temperature and relative humidity, and then is linearly fitted to the data-driven model. Afterward, the uncertainty set is constructed based on the historical forecast error to the weather information, i.e., the differences between forecast and real-measured values. This uncertainty set can be further clustered by the k-means algorithm, and PCA combined with KDE can return the polyhedral-shaped applied to the RMPC. The optimization problem at each control horizon is solved with the help of the affine disturbance feedback (ADF). The contribution of this paper is summarized as follows:

- A novel hybrid model for the multi-zone building which considers both temperature and relative humidity within each individual zone;
- A novel data-driven control approach for the multi-zone building's model.

2. HYBRID MODEL FORMULATION & CONTROL

2.1 Physics-based model construction

The BRCM MATLAB toolbox is used for finding the temperature values within the multi-zone building (Sturzenegger et al., 2014). BRCM can generate the linear resistance-capacitance models from self-designed building geometry construction. The following dynamic multi-input multi-output system can be returned:

$$x_{t+1} = Ax_t + B_u u_t + B_v v_t + B_w w_t \tag{1}$$

where A is the state matrix that correlates state variables x_t to SSM. The state variables returned from BRCM are room temperature, wall temperature, floor temperature, and ceil temperature. B_u, B_v, B_w are the control input matrix, disturbance matrix, and uncertainty matrix, respectively, corresponding to u_t, v_t, $w_{t,}$ which are control input, disturbances, and uncertainty. The control inputs include heater, radiator, humidifiers, and dehumidifiers; the disturbances are from ambient temperature and ambient relative humidity conditions. Uncertainties are the forecasted error of temperature and relative humidity. In order to extend this SSM with humidity values, relative humidity within each room is calculated based on the air dynamic within the building (Cengel, 1997). In work by Rentel-Gomez and Velez-Reyes (2001), several assumptions are made in the derivation of the physics-based model: (i) ideal gas behavior, (ii) perfect mixing, (iii) constant pressure process, (iv) negligible infiltration and exfiltration effects. Based on assumption (iv), the water vapor can be assumed to be exclusively adjusted by the amount of air supply, humidifiers, and dehumidifiers.
The mass of airflow is initially found as:

$$m_{air,t-1} = \frac{Q_{t-1}}{c_p \Delta T} \tag{2}$$

ΔT is calculated as follows:

$$\Delta T = \max\left(\left(T_{room,t} + \delta T - T_{air,t}\right), 0\right) \tag{3}$$

Unlike in previous research, $m_{air,t-1}$ is not assumed a constant because the simulation process is conducted in the winter season. The constant intake airflow rate implies that the room is constantly exchanging the air with a colder ambient environment. The heater, most of the time, is active to maintain the room. In this case, we assume the difference between the room temperature and heated air from the air heating unit (AHU) is constant. Subsequently, the heating airflow can be turned off when heating is unnecessary. When the mass of airflow is calculated, the mass of water vapor brought by airflow can be found by the following equation:

$$m_{AC,in,t-1} = \rho_{AC,in,t-1} \cdot RH_{out,t-1} \cdot \frac{m_{air,t-1}}{\rho_{air}} \tag{4}$$

And so can be found the mass of water vapor taken away by airflow:

$$m_{AC,out,t-1} = \rho_{water,sat,t-1} \cdot RH_{t-1} \cdot \frac{m_{air,t-1}}{\rho_{air}} \tag{5}$$

where saturated vapor density (SVD) values are found through equation f, which is a linear equation of SVD values over temperature (T) expressed as follows:

$$\rho_{water} = f(T) = 1.0272T - 1.8959 \tag{6}$$

Afterward, the mass of water vapor stored in each room can be found as:

$$\begin{aligned} m_{water,t} = {} & \rho_{water,sat,t-1} \cdot RH_{t-1} \cdot V_{room} + m_{hum,t} + \\ & m_{AC,in,t-1} - m_{dehum,t} - m_{AC,out,t-1} \end{aligned} \tag{7}$$

RH values within each room at t can then be found as the ratio of absolute and saturated water vapor density:

$$\rho_{abs,t} = \frac{m_{water,t}}{V_{room}},\ \rho_{sat,t} = f\left(T_{room,t}\right),\ RH_t = \frac{\rho_{abs,t}}{\rho_{sat,t}} \tag{8}$$

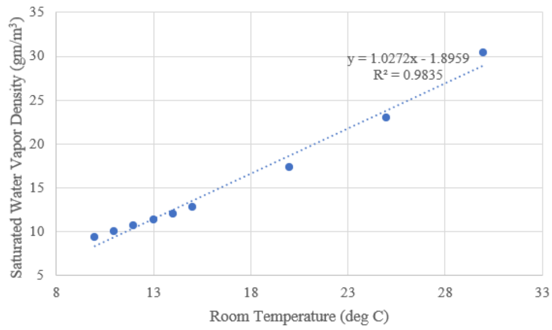

Fig. 1. Linearized saturate relative humidity equation with room temperature. The blue dots are the non-linear equation retrieved from (Nave, 2012).

At this point, the RH values within each room can be found based on the room temperature, control input, and room size.

2.2 System identification

The relative humidity is added to SSM through the system identification toolbox found in MATLAB. We assume that the in-room relative humidity has a negligible impact on the wall, floor, and ceil temperature values based on the assumption of "negligible wall and thermal storage" (Rentel-Gomez and Velez-Reyes, 2001). Following the assumption, we can reduce the size of the system identification model, thereby cutting the required computational time. With trained and test datasets, one room's values have been selected and demonstrated in Fig. 2. The mean error values of the System Identification result have been summarized in Table I and Table II.

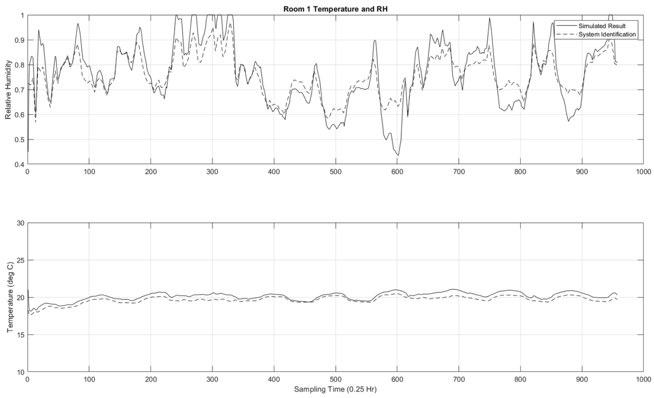

Fig. 2. System identification on testing data.

Table 1. Mean absolute percentage error (MAPE) of system identification of training data

	RH	Temperature
Room 1	6.37 %	1.24 %
Room 2	4.89 %	1.04 %
Room 3	6.34 %	1.24 %
Room 4	6.53 %	1.25 %
Room 5	6.80 %	1.30 %

Table 2. Mean absolute percentage error (MAPE) of system identification of testing data

	RH	Temperature
Room 1	7.33 %	2.38 %
Room 2	3.92 %	2.00 %
Room 3	7.34 %	2.37 %
Room 4	7.29 %	2.40 %
Room 5	7.32 %	2.50 %

As demonstrated in Table I and Table II, the MAPE values for temperature testing data are between 2.00% to 2.50%, and for relative humidity are between 3.92% to 7.34%. The error values are relatively close to those in work by Yang et al. (2018), indicating a good agreement between the linearized SSM and the non-linear model. Therefore, we can use this SSM to formulate the following control problem.

2.3 Control strategy development

Disjunctive uncertainty sets are built for learning the trend of the uncertainty data (Ning and You, 2017, 2018). To tackle forecast uncertainties' complex disjoint-set data structure (Fay and Ringwood, 2010), the k-means clustering method is adopted in this work to cluster the uncertainty into multiple groups. First, normalization of the uncertainty data is recommended, shown in (10), to facilitate the convergence of Newton's algorithm, which will be used in K-means (Bottou and Bengio, 1995).

$$w_0 = w - 1\mu_0^T \tag{9}$$

The groups are identified by minimizing the sum of intracluster variances, i.e., squared Euclidean Distance shown below:

$$D^* = \arg\min\left(\sum_{i=1}^{k}\sum_{w\in D_i}\left\|w-\mu_i\right\|^2\right) \tag{10}$$

Despite multiple groups of uncertainty data, the traditional norm-based uncertainty set cannot be applied directly to deal with the uncertainty data due to its varied structure and complexity. Therefore, PCA and KDE are used here for handling the data with polyhedral shapes. PCA can then maximize the variance of the uncertainty under the same scale. The covariance matrix can be approximated as

$$S_i = \frac{1}{N-1} w_i^T w_i \tag{11}$$

As the covariance matrix, S_i can be further decomposed as $S_i = Q_i \Lambda_i Q_i^T$, where Q_i's column contains all the eigenvectors, corresponding to the eigenvalues stored in the diagonal matrix Λ_i. The individual eigenvalue will represent the variance of this axis if data is projected on this eigenvector.

Finally, it can be further studied the distributional information of the uncertainty dataset within each component j within the cluster k via the KDE approach:

$$f_{j,k} = \frac{1}{N}\sum_{n=1}^{N} K(\xi_{j,k}, p_{j,k}^{(n)}) \tag{12}$$

With the probability density function, the cumulative density function will be written as follows:

$$F_{j,k}^{-1}(\alpha) = \min\{\xi_{j,k} \mid F_{j,k}(\xi_{j,k} \geq \alpha)\} \tag{13}$$

where α is the pre-specified small quantile parameter, ranging from 0 to 0.5, and ξ is the inferred latent variable. The uncertainty set W_k within cluster k can be formulated under the introduction of forward and backward deviation variables z^+ and z^- (Ning and You, 2018, 2019):

$$\mathbb{W}^k = \left\{ \mathbf{w}^k \in R^H \,\middle|\, \begin{array}{l} \mathbf{w}^k = \hat{\boldsymbol{\mu}}_k + Q_k \xi_k,\ \xi_k = \underline{\xi}_k z^- + \overline{\xi}_k z^+ \\ \mathbf{0} \le z^+, z^- \le \mathbf{1},\ z^+ + z^- \le \mathbf{1},\ \mathbf{1}^T\left(z^+ + z^-\right) \le \Gamma \\ \underline{\xi} = \left[\hat{F}_{1,k}^{-1}(\alpha),...,\hat{F}_{1,k}^{-1}(\alpha)\right]^T \\ \overline{\xi} = \left[\hat{F}_{1,k}^{-1}(1-\alpha),...,\hat{F}_{1,k}^{-1}(1-\alpha)\right]^T \end{array} \right\} \tag{14}$$

3. CONTROL STRATEGY

After the acquisition of the SSM required for MPC and uncertainty sets, the next step is to develop the optimization problem to get the control strategy to the multi-zone building. To ensure the tractability of the RMPC optimization problem, ADF is adopted to get control input u_t based on past disturbances. The equation is expressed as follows (Goulart et al., 2006):

$$u_i = h_i + \sum_{j=0}^{i-1} M_{i,j} w_j,\ \forall w \in \mathbb{W}^k \tag{15}$$

where M is regulated as follows:

$$M = \begin{bmatrix} 0 & \cdots & \cdots & 0 \\ M_{1,0} & 0 & \cdots & 0 \\ \vdots & \vdots & \ddots & \vdots \\ M_{H,0} & M_{H,1} & \cdots & 0 \end{bmatrix} \tag{16}$$

Only the first u_0 will be applied for the control to the model, and the rest will be discarded (Chen et al., 2021). The optimization problem with ADF can be formulated as follows:

$$\begin{aligned} &\min \sum_{i \in B_u} c_i u_i + \lambda^T L \lambda \\ &\text{s.t. } F_u[Mw + h] \le f_u, && \forall w \in \mathbb{W}^k \\ &\quad F_x[Ax_0 + B_u h + B_v v + (B_w + B_u M)w] \le f_x + \lambda, && \forall w \in \mathbb{W}^k \end{aligned} \tag{17}$$

Where F_x, F_u, f_x, f_u represent the state variable constraints matrix, control input constraints matrix, constraints for state variables, and constraints for the input. L is the weighted cost matrix that penalizes the violation of the constraints. Λ is the slack variable that allows some extent of violation to the hard constraints.

4. CASE STUDY

4.1 Problem statement

In this study, the single-floor multi-zone building located in Ithaca, New York, USA, is selected for the simulation of close-loop data-driven RMPC to control the temperature and relative humidity in each individual room. The self-constructed floor plan can be referred to Fig. 3. The forecasted weather data is retrieved from Herzmann et al. (2004); the actual measured data is retrieved from Diamond et al. (2013). The constraints for the control conditions are: For the room temperature should be within 15 ℃ to 25 ℃, and relative humidity should sit between 30 % to 60 %, according to ASHRAE Standard 62-2001. The solver GUROBI in Python is adopted, and all computations are performed on XPS 17 9700 equipped with Intel Core i7-10875 CPU @ 2.30 GHz and 16 GB of RAM.

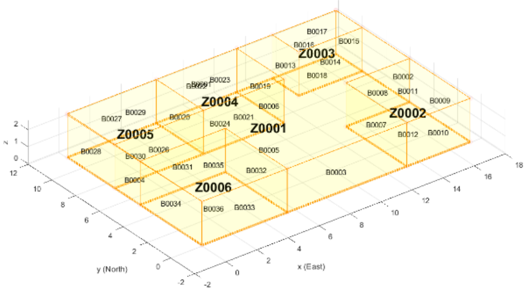

Fig. 3. 3-D Modeling of Multi-Zone House in BRCM

4.2 Results and discussion

The model was simulated in Ithaca, New York, from 0:00 AM, November 1st, 2016, to 0:00 AM, on November 8th, 2016, ranging from precisely one week. The initial conditions for temperature values in all rooms are 21 ℃, and RH values are 40 %. The simulation result is shown in Fig. 4. Both CEMPC and RMPC violate the constraints more severely. CEMPC, which only considers the deterministic conditions, fails to compose the strategy against the prediction error from ambient temperature and relative humidity. Meanwhile, the RMPC fails to obey the relative humidity constraints, indicating an irregular shape of the uncertainty data of relative humidity. The violation of relative humidity mostly occurs when heating is opened to maintain the room temperature, and air circulation will take away the water vapor within the room and bring more dry air from outside. The RMPC does not use any power from humidifiers or dehumidifiers to control the relative humidity. This explains that this strategy manages to achieve the lowest power consumption, suggesting it favors more energy-saving options and receives expensive violation penalties instead of following the settled constraints. On the other hand, the rest three control strategies can be more conservative in maintaining both temperature and relative humidity within the constraints. KMDDRMPC will be the most conservative one since there is nearly no violation, whereas it will have the highest power consumption across all control methods. Furthermore, though there are slightly more violation cases and more computation time, KMPKDDRMPC will draw significantly less power in controlling the temperature and relative humidity compared to KMDDRMPC and PKDDRMPC. Overall, our proposed KMPKDDRMPC saves 9.8 % of energy usage compared to PKDDRMPC and 17.9 % compared to KMDDRMPC.

Another observation is the control benefits from disjunctive uncertainty sets. For temperature control, KM-PKDDRMPC manages to lower the violation frequency and reduce the energy usage compared to PKDDRMPC. Similarly, for relative humidity control, KM-PKDDRMPC uses less energy to maintain relative humidity within a comfortable range than PKDDRMPC. KM-DDRMPC also shows an advantage in controlling relative humidity compared to RMPC by significantly lowering the violation frequency. Therefore, it is safe to acknowledge that disjunctive uncertainty sets can help improve the controller’s ability to hedge against uncertainty disturbances.

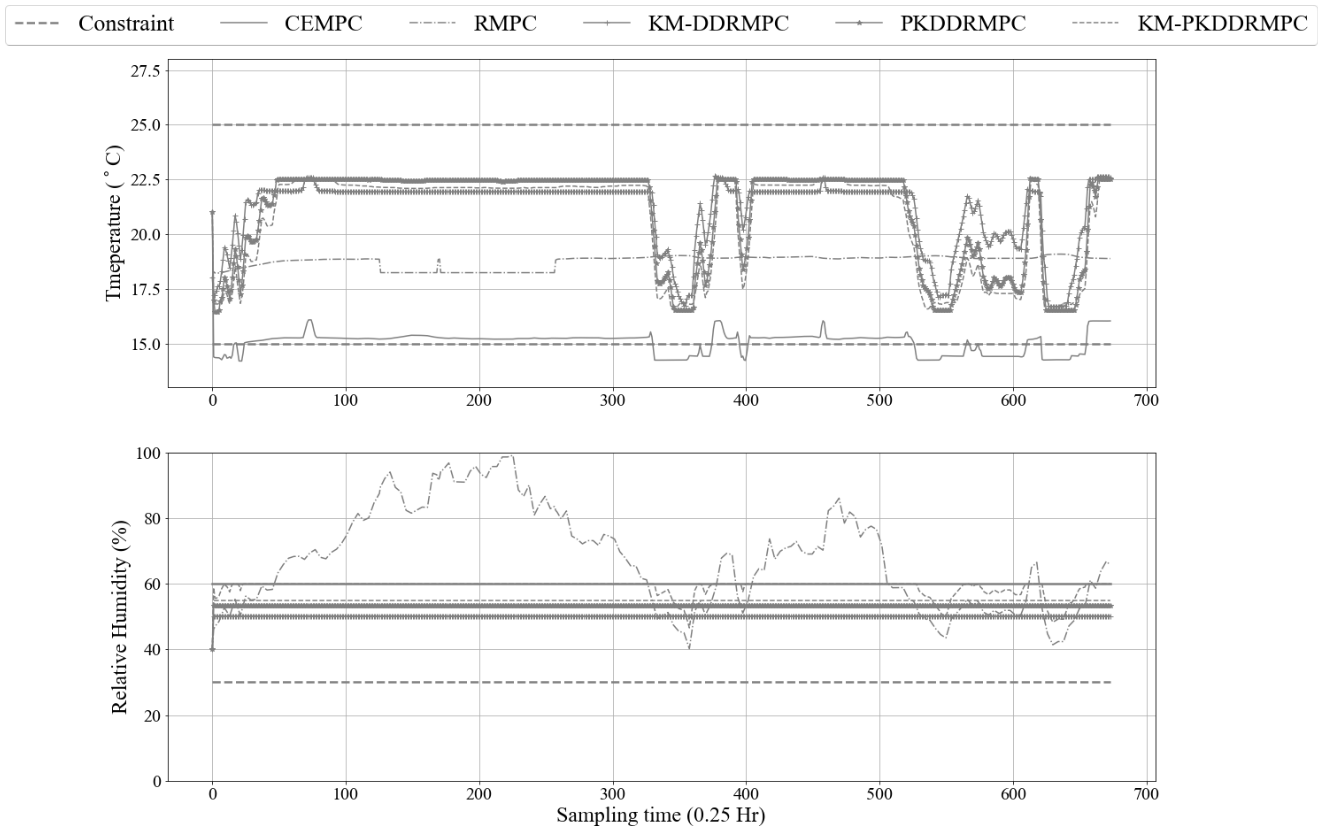

Figure 4. Multi-zone building control profile in Ithaca, New York, in the first week of November 2016

The major novelty of this paper is that we build data-driven disjunctive uncertainty based on the k-mean clustering algorithm, and we can observe the control benefits from disjunctive uncertainty sets. For temperature control, KMPKDDRMPC manages to lower the violation rate by reducing the energy usage compared to PKDDRMPC. Similarly, for relative humidity control, KMPKDDRMPC uses less energy in maintaining relative humidity within a comfortable range compared to PKDDRMPC. KMDDRMPC also shows an advantage in controlling relative humidity compared to RMPC by significantly lowering the violation rate. Therefore, it is safe to acknowledge that disjunctive uncertainty sets can help improve the control's ability to hedge against noise disturbances while being applied under stochastic conditions.

Compared with other MPC's, the optimal control problem is more sophisticated in our proposed framework because a considerable number of Lagrange multipliers have been introduced to transform the infinite-dimensional problem into its robust counterpart. Despite this, the computation is still trivial considering that all constraints can still be reformulated in the form of linear inequalities and equalities contributed from ADF policy, which can be readily solved by convex programming techniques. The average CPU time for our proposed framework is only 1.23 s, which is totally acceptable in real-life applications because it is sufficient to finish the optimization procedure within the sampling interval of 15 minutes.

5. CONCLUSION

In this work, we developed a KM-PKDDRMPC framework for the multi-zone building SSM, which includes indoor temperature and relative humidity control and is constructed from a hybrid approach. In order to maintain temperature and relative humidity within the comfortable range, KM-PKDDRMPC is capable of handling the uncertainty sets from temperature and relative humidity forecast. The steady-state system with relative humidity is constructed based on the physics-based model and linearized with the help of system identification. Then the optimization problem can be further developed with the SSM and disjunctive uncertainty sets. The proposed KM-PKDDRMPC was compared with the CEMPC and other MPC strategies, including RMPC, KM-DDRMPC, PKDDRMPC. The result demonstrated that the proposed KM-PKDDRMPC had outperformed the rest from the overall perspective, using 17.9 % less power consumption than KMDDRMPC and 9.8 % fewer than PKDDRMPC. Though CEMPC and RMPC used less power than other RMPCs, the high violation rate would exclude them from the final consideration for the practical application.

REFERENCES

American Society of Heating, Refrigerating and Air Conditioning Engineers. (2001). *Standard 62-2001, Ventilation for acceptable indoor air quality.* The Society, New York.

Baughman, A. V. & Arens, E. A. (1996). Indoor humidity and human health - Part I: Literature review of health effects of humidity-influenced indoor pollutants. *ASHRAE Transactions,* 102(1), 193-211.

Bottou, L. & Bengio, Y. Convergence properties of the k-means algorithms. (1995). *Advances in neural information processing systems,* 585-592.

Cengel, Y. A. (1997). *Introduction to thermodynamics and heat transfer*: McGraw-Hill, New York.

Chen, W.-H., Shang, C., Zhu, S., et al. (2021). Data-driven robust model predictive control framework for stem water potential regulation and irrigation in water management. *Control Engineering Practice*, 113, 104841.

Chen, W.-H., & You, F. (2021). Smart greenhouse control under harsh climate conditions based on data-driven robust model predictive control with principal component analysis and kernel density estimation. *Journal of Process Control*, 107, 103-113.

Chen, W.-H., & You, F. (2022). Semiclosed Greenhouse Climate Control Under Uncertainty via Machine Learning and Data-Driven Robust Model Predictive Control. *IEEE Transactions on Control Systems Technology*, 30, 1186-1197.

D'agostino, D., Zangheri, P. & Castellazzi, L. (2017). Towards nearly zero energy buildings in Europe: A focus on retrofit in non-residential buildings. *Energies,* 10(1), 117.

Diamond, H. J., Karl, T. R., Palecki, M. A., Baker, C. B., Bell, J. E., Leeper, R. D., Easterling, D. R., Lawrimore, J. H., Meyers, T. P., Helfert, M. R., Goodge, G. & Thorne, P. W. (2013). U.S. Climate Reference Network after One Decade of Operations: Status and Assessment. *Bulletin of the American Meteorological Society,* 94(4), 485-498.

EIA. (2019). *Use of energy explained*. U.S. Energy Information Administration.

Fay, D. & Ringwood, J. V. (2010). On the Influence of Weather Forecast Errors in Short-Term Load Forecasting Models. *IEEE Transactions on Power Systems,* 25(3), 1751-1758.

Goulart, P. J., Kerrigan, E. C. & Maciejowski, J. M. (2006). Optimization over state feedback policies for robust control with constraints. *Automatica,* 42(4), 523-533.

Herzmann, D., Arritt, R. & Todey, D. (2004). *Iowa environmental mesonet.* Iowa State.

Jia, R., & You, F. (2020). Multi‐stage economic model predictive control for a gold cyanidation leaching process under uncertainty. *AIChE Journal*, 67, e17043

Johnson, M. A. & Moradi, M. H. (2005). *PID control*: Springer.

Kiam Heong, A., Chong, G. & Yun, L. (2005). PID control system analysis, design, and technology. *IEEE Transactions on Control Systems Technology,* 13(4), 559-576.

Ma, Y., Borrelli, F., Hencey, B., Coffey, B., Bengea, S. & Haves, P. (2012). Model Predictive Control for the Operation of Building Cooling Systems. *IEEE Transactions on Control Systems Technology,* 20(3), 796-803.

Marszal, A. J., Heiselberg, P., Bourrelle, J. S., Musall, E., Voss, K., Sartori, I. & Napolitano, A. (2011). Zero Energy Building – A review of definitions and calculation methodologies. *Energy and Buildings,* 43(4), 971-979.

Morosan, P.-D., Bourdais, R., Dumur, D. & Buisson, J. (2011). Distributed MPC for Multi-zone Temperature Regulation with Coupled Constraints. *IFAC Proceedings,* 44, 1552-1557.

Nave, C. R. (2012). Hyperphysics, Georgia State University. *Canada*.

Ning, C. & You, F. (2017). Data-Driven Adaptive Nested Robust Optimization: General Modeling Framework and Efficient Computational Algorithm for Decision Making Under Uncertainty. *AIChE Journal*, 63, 3790-3817.

Ning, C. & You, F. (2018). Data-driven decision making under uncertainty integrating robust optimization with principal component analysis and kernel smoothing methods. *Computers & Chemical Engineering,* 112, 190-210.

Ning, C. & You, F. (2018). Data-driven decision making under uncertainty integrating robust optimization with principal component analysis and kernel smoothing methods. *Computers & Chemical Engineering*, 112, 190 – 210.

Ning, C. & You, F. (2019). Optimization under uncertainty in the era of big data and deep learning: When machine learning meets mathematical programming. *Computers & Chemical Engineering*, 125, 434-448.

Ning, C. & You, F. (2021). Online learning based risk-averse stochastic MPC of constrained linear uncertain systems. *Automatica*, 125, 109402.

Oldewurtel, F., Parisio, A., Jones, C. N., Gyalistras, D., Gwerder, M., Stauch, V., Lehmann, B. & Morari, M. (2012). Use of model predictive control and weather forecasts for energy efficient building climate control. *Energy and Buildings,* 45, 15-27.

Prívara, S., Široký, J., Ferkl, L. & Cigler, J. (2011). Model predictive control of a building heating system: The first experience. *Energy and Buildings,* 43(2), 564-572.

Rentel-Gomez, C. & Velez-Reyes, M. (2001). Decoupled control of temperature and relative humidity using a variable-air-volume HVAC system and non-interacting control. *Proceedings of IEEE International Conference on Control Applications,* 2001. 1147-1151.

Shaikh, P. H., Nor, N. B. M., Nallagownden, P., Elamvazuthi, I. & Ibrahim, T. (2014). A review on optimized control systems for building energy and comfort management of smart sustainable buildings. *Renewable and Sustainable Energy Reviews,* 34, 409-429.

Shang, C., Chen, W.-H., Stroock, A. D., et al., (2020). Robust Model Predictive Control of Irrigation Systems With Active Uncertainty Learning and Data Analytics. *IEEE Transactions on Control Systems Technology*, 28, 1493-1504.

Shang, C., Huang, X., & You, F. (2017). Data-driven robust optimization based on kernel learning. *Computers & Chemical Engineering*, 106, 464-479.

Shang, C., & You, F. (2019). A data-driven robust optimization approach to scenario-based stochastic model predictive control. *Journal of Process Control*, 75, 24-39.

Shang, C., & You, F. (2019). Data Analytics and Machine Learning for Smart Process Manufacturing: Recent Advances and Perspectives in the Big Data Era. *Engineering*, 5, 1010-1016.

Shi, G., Liu, D. & Wei, Q. (2016). Energy consumption prediction of office buildings based on echo state networks. *Neurocomputing,* 216, 478-488.

Široký, J., Oldewurtel, F., Cigler, J. et al. (2011). Experimental analysis of model predictive control for an energy efficient building heating system. *Applied Energy,* 88(9), 3079-3087.

Sturzenegger, D., Gyalistras, D., Semeraro, V., Morari, M. & Smith, R. S. (2014). BRCM Matlab Toolbox: Model generation for model predictive building control. *2014 American Control Conference,* 4-6 June 2014, 1063-1069.

Yang, R. & Wang, L. (2013). Multi-zone building energy management using intelligent control and optimization. *Sustainable Cities and Society,* 6, 16-21.

Yang, S., Wan, M. P., Ng, B. F., et al. (2018). A state-space thermal model incorporating thermal comfort for model predictive control in buildings. *Energy and Buildings,* 170, 25-39.

Yun, L., Kiam Heong, A. & Chong, G. C. Y. (2006). PID control system analysis and design. *IEEE Control Systems Magazine,* 26, 32-41.

Zingano, B. W. (2001). A discussion on thermal comfort with reference to bath water temperature to deduce a midpoint of the thermal comfort temperature zone. *Renewable Energy,* 23, 41-47.